Femtosecond Dynamics of $Fe(CO)_5$ Photodissociation at 267 nm Studied by Transient Ionization

S. A. Trushin,[†,‡] W. Fuss,*[,†] K. L. Kompa,[†] and W. E. Schmid[†]

Max-Planck-Institut für Quantenoptik, D-85740 Garching, Germany, and B.I. Stepanov Institute of Physics, Belarus Academy of Sciences, 220602 Minsk, Belarus

Received: July 20, 1999; In Final Form: December 23, 1999

We found five consecutive processes with time constants 21, 15, 30, 47, and 3300 fs in $Fe(CO)_5$ after excitation at 267 nm in the gas phase. The first four represent a continuous pathway of the molecule from the Franck−Condon region down to the lowest singlet state (S_0) of $Fe(CO)_4$ through a chain of Jahn−Teller-induced conical intersections. The motion before dissociation initially involves more than one of the equatorial ligands, but then eliminates only one CO. The product $Fe(CO)_4$ is initially generated in its first excited singlet state S_1, then it relaxes to S_0 in 47 fs via a triply degenerate conical intersection at tetrahedral geometry. The pathway for this process involves pseudorotation of the ligands. The fifth step is assigned to thermal elimination of a second CO. Intersystem crossing to the triplet ground states of $Fe(CO)_4$ and $Fe(CO)_3$ takes more than 500 ps.

1. Introduction

It has long been known that metal carbonyl compounds eliminate a CO group on photolysis in the UV.[1,2] The products as well as other unsaturated transition metal complexes play an important role in, for example, CH activation.[3] It is not known, however, whether this reaction proceeds in the form of simple bond breaking on directly repulsive potential energy surfaces, such as is the case in organic iodides for instance. Some of the unsaturated complexes produced are triplets in their ground state, and it is an open question where intersystem crossing occurs. Modern femtosecond spectroscopy can investigate the dynamics during dissociation and yields information about the potential energy surfaces. The simple metal carbonyls offer themselves as prototype molecules.

A number of recent studies using femtosecond laser pump−probe spectroscopy are focused on the photodissociation dynamics of metal carbonyls in the gas phase.[4−10] After photolysis of $Fe(CO)_5$, Zewail and co-workers investigated the structure of the end products ($Fe(CO)_2$ and Fe(CO) in this case) by electron diffraction;[5] the time resolution (2 ps) was not yet sufficient to detect intermediates during dissociation. As known from previous work without time resolution, in the gas phase the number of CO ligands eliminated and hence the end product depend on the photon energy.[11] Baumert, Gerber, and co-workers investigated with femtosecond resolution the question of how synchronously the metal−ligand bonds are cleaved.[6,7] They claimed that four carbonyl groups are eliminated concertedly, while the molecule moves along a single repulsive potential energy curve with no stationary intermediates.

On the basis of previous and new evidence, we point out that only the first CO is split off photochemically (i.e., bond breaking begins in the excited state) in a time below 100 fs, whereas already the second elimination takes place in the S_0 of $Fe(CO)_4$ and requires a much longer time (3.3 ps with our wavelength of 267 nm). Intersystem crossing does not take place within the investigated time range of 500 ps.

Since hot ground state reactions are usually suppressed in the condensed phase by rapid cooling, only the photochemical step should be observable in this case. In fact, it has long been known that in solution only one CO is split off by irradiation of $Fe(CO)_5$ and other metal carbonyls at any UV wavelength.[2,12] To explain the large quantum yield of this photochemical step, Wrighton and Geoffroy suggested that the process occurs on a directly repulsive potential energy curve, which is provided by a d−d ("ligand field", LF) excited state.[1,2] They assumed it is populated by direct optical excitation. But since the metal-to-ligand charge-transfer ($d \rightarrow \pi^*_{CO}$, MLCT) states carry more intensity in the UV spectrum and will be preferentially excited, one should rather consider relaxation from an MLCT to an LF state. It is not obvious from the outset how such a relaxation can be as fast as observed. In addition to answering such questions, we show that the process is even richer in details, comprising not only several electronic states but also changes of direction in the coordinate space. We claim that the primary product is $Fe(CO)_4$ in its first excited singlet state S_1 which relaxes via pseudorotation to S_0. All the pathway is continuous, crossing over from state to state via a chain of conical intersections which are induced by the Jahn−Teller effect. Before $Fe(CO)_4$ can proceed by intersystem crossing to the triplet ground state, under our conditions it dissociates due to excess vibrational energy to singlet $Fe(CO)_3$. From the observations, we can derive many qualitative features of the potential energy surfaces.

In previous work, an upper bound of the lifetime (0.5 ps) of excited $Fe(CO)_5$ has been estimated from the yield of two-photon ionization.[13] Information about the dynamics and the potential energy surfaces (PES) can also be deduced from the energy of the photofragments.[13,14] A statistical model has been suggested for such energy distributions.[14−16] Of particular interest is a comparison with infrared observation of the primary photoproducts with nanosecond time resolution[17−20] and of the

* Corresponding author. E-mail: w.fuss@mpq.mpg.de. Fax: +49-89-32905-200.
[†] Max-Planck-Institut für Quantenoptik.
[‡] Belarus Academy of Sciences.

10.1021/jp992474u CCC: $19.00
Published on Web 02/18/2000

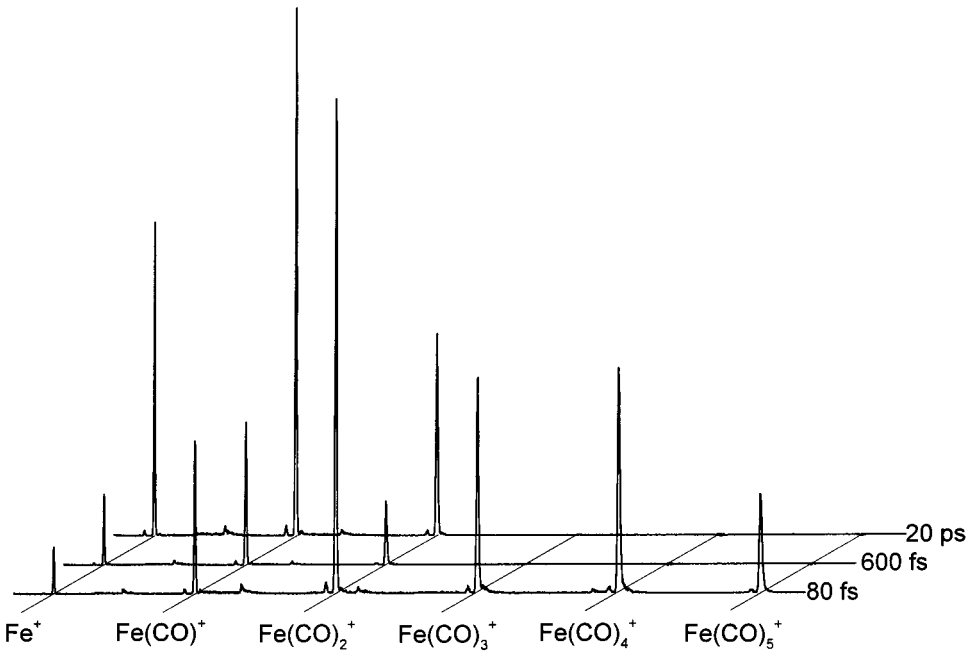

Figure 1. Transient time-of-flight spectra obtained after irradiation of $Fe(CO)_5$ with 267 nm pump pulses and 800 nm probe pulses delayed by 80, 600, and 20000 fs. The background, which is due to ionization by the probe pulses alone, is subtracted.

photochemistry in solution[2] and in a matrix.[21] Daniel and coworkers calculated potential energy curves for dissociation of $Fe(CO)_5$[22−25] and the related carbonyl hydride $H_2Fe(CO)_4$.[25]

Several other high-level calculations investigated the energy of the excited states of $Fe(CO)_5$ at the ground state geometry and the energies and structure of some states of $Fe(CO)_4$.[26−28] A very recent ab initio calculation suggests some reassignments of UV bands and changes in the sequence of excited states.[29] $Fe(CO)_5$ is of trigonal bipyramidal shape (symmetry D_{3h}). $Fe(CO)_4$ is not far from this geometry, but with one equatorial ligand removed and the angle between the axial ligands decreased to some extent (symmetry C_{2v}).[21,26,27] It has a triplet ground state.[21] The gas-phase UV spectrum of $Fe(CO)_5$ is given in ref 30 and the ionization energy (7.9 eV) in ref 31. The energies required for the consecutive dissociation steps have been reported for neutral $Fe(CO)_5$ (1.78, 0.43, 1.08, 1.17, and 1.69 eV[14]) and its cation (1.4, 1.1, 0.7, 1.5, and 1.6 eV[32]). Further previous related work is reviewed in.[7]

2. Experimental Section

Our experiment follows standard femtosecond pump−probe techniques with photoionization mass spectrometry using a Ti:sapphire oscillator−amplifier system and a linear time-of-flight (TOF) mass spectrometer (MS). The setup is described in detail elsewhere.[33−36] Briefly, the third harmonic at 267 nm (pulse length 145 fs) was used for pumping and the fundamental at 800 nm (110 fs) for ionization, probing with varying delay. In contrast to the pump radiation, the probe pulses (energy around 300 μJ) were focused (focal length of 100 cm), resulting in a peak intensity of about 2×10^{12} W cm^{-2} (pump intensity about 10^9 W cm^{-2}). The probe beam polarization was set by a half-wave plate at an angle of 54.7° (magic angle) relative to the pump beam polarization. This is known to eliminate the time-dependent effects induced by the rotation of the molecules. In later measurements, we also checked for anisotropy decay, comparing the signals with the probe parallel and perpendicular to the pump. But the time behavior was identical.

The time zero was determined as the maximum of the transient ion signal for Xe, which is due to pure nonresonant (2 + 2) multiphoton ionization. The instrumental function (i.e., the pump−probe correlation function) was measured by ionization of $Cr(CO)_6$ with detection of the parent ion; the lifetime of excited $Cr(CO)_6$ is short enough that it does not distort this function and causes only a known small delay (22 fs).[8] This molecule has the same order of the ionization process (1 pump + 3 probe photons) as $Fe(CO)_5$. Two ion signals (normally the $Cr(CO)_6^+$ and one of the Fe-containing ion peaks) were recorded simultaneously by means of two boxcar integrators. This method provided synchronization of different scans with an accuracy of ±2 fs. In our setup, ions between mass 56 (Fe^+) and 196 amu ($Fe(CO)_5^+$) have times of flight from 3 to 5.7 μs and give rise to peaks 7−10 ns wide. It is worth noting that ions produced by delayed thermal dissociation of a heavier ion in times shorter than this width cannot be distinguished from those produced promptly. For a detailed discussion see.[36]

The signals produced by pump and probe pulses alone (less than 1% of the maximum of each transient signal) were subtracted from the measured signals.

The $Fe(CO)_5$ (Fluka, 99%, used after degassing), $Cr(CO)_6$ (Fluka, 99%), and Xe (Linde, >99.9%) were fed into the ionization chamber through three separate leak valves adjusted to produce pressures of 10^{-7} mbar (10^{-5} mbar for Xe). All measurements were performed at room temperature.

3. Results

Mass spectra for three different pump−probe delay times are shown in Figure 1. At early delay times (less than 100 fs) all six Fe-containing ionic fragments show transient signals. With longer delays the heavy fragments disappear, but light fragments persist or show up. The mass spectrum practically does not change any more after 300 fs, although the total ion signal keeps increasing, asymptotically reaching its maximum at about 20 ps. Thereafter, the signals are constant up to the investigated time of 500 ps.

The signals measured at the parent and all fragments ions are shown in Figures 2 and 3 on different time scales. The three heaviest ions, $Fe(CO)_n^+$, $n = 5, 4, 3$, only show an initial spike at early pump−probe delay times and practically disappear after

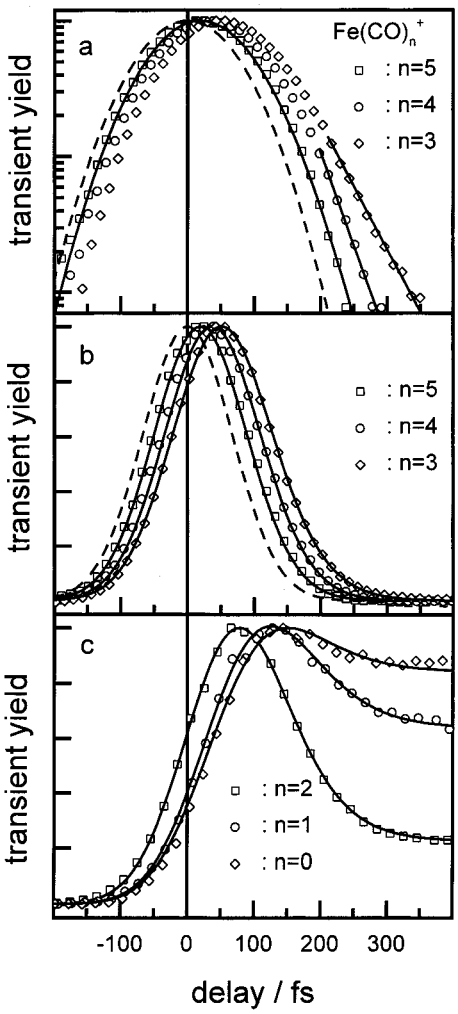

Figure 2. Early pump−probe transients $Fe(CO)_n^+$, $n = 5, ..., 0$ in 267 nm photolysis of iron pentacarbonyl probed by delayed ionization at 800 nm. The symbols show the experimental data. The scale is singly logarithmic in (a) and linear in (b) for the same data. The broken curve in (a, b) is the response function measured (see text) and calculated for pump and probe pulses of 145 and 110 fs width, respectively, it being assumed that three probe photons are used for ionization. The straight lines in (a) are singly exponential functions with time constants of 30 ± 3 fs for $Fe(CO)_4^+$ and 47 ± 5 fs for $Fe(CO)_3^+$. The solid curves are from the multiexponential simulation (see text) convoluted with the pump and probe pulses. The data for the parent ion are well fitted to a convoluted singly exponential function with time constant of 21 ± 2 fs.

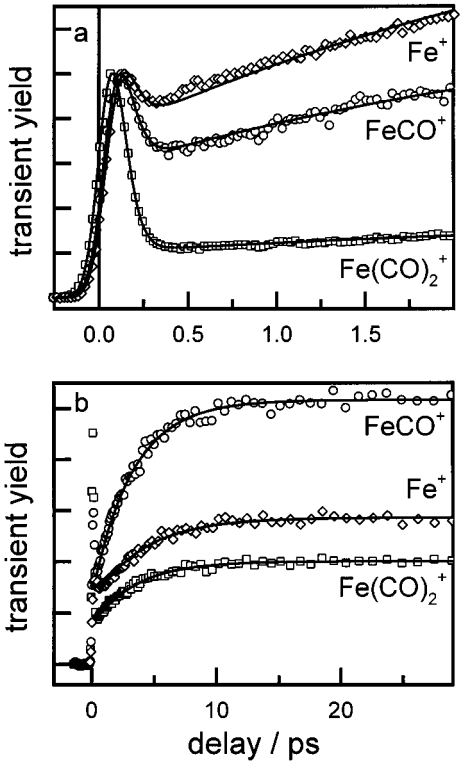

Figure 3. Long-lived pump−probe transients $Fe(CO)_n^+$, $n = 2, 1, 0$ in 267 nm photolysis of iron pentacarbonyl probed by delayed ionization at 800 nm. Note the different time scales in (a) and (b). Symbols show the experimental data. The curves in (b) are singly exponential functions. They all rise with the same time constant of 3300 ± 300 fs. The curves in (a) are from the multiexponential simulation (see text) convoluted with the pump and probe pulses. In the range of 300−2000 fs, there are no oscillations of the kind typical of the long-lived transients in UV photolysis of $M(CO)_6$, M = Cr, Mo, W.[8,9]

300 fs. However, they do not coincide and their temporal behavior can be clearly distinguished. Note that the absolute time zero was determined from the maximum of the transient ion signal for Xe (section 2). The dashed lines in Figure 2 a and b show the measured response function (section 2). It has a width of 158 fs. The parent ion $Fe(CO)_5^+$ shows no asymmetry and fits well to a Gaussian function with a width of 165 fs, but with a 20 fs shift from the zero point. This shift can be well reproduced (solid lines in the figures) by fitting the experimental data to a single-exponential function with a time constant of 21 ± 2 fs convoluted with the response function. The transients $Fe(CO)_4^+$ and $Fe(CO)_3^+$ are noticeably delayed in relation to the parent ion; their maxima are at 40 and 50 fs, respectively. Moreover, these signals are asymmetric and their tails can be fitted (broken lines) to single exponentials with time constants of 30 ± 3 and 47 ± 5 fs, respectively, as shown in Figure 2a.

Compared with the heavier ions, the light ions $Fe(CO)_n^+$, $n = 2, 1, 0$, show rather different transient kinetics. The sharp spike at the early time (Figure 2c) is followed by a short dip and a subsequent rise for times greater than 300 fs (parts a and b of Figure 3). The transients are peaked at 80, 125, and 145 fs for $n = 2, 1, 0$, respectively. It is important that the decay time constant (47 ± 5 fs) derived from a singly exponential fit to the tail of these ions agrees with that of $Fe(CO)_3^+$. It is also meaningful that all three light fragments show secondary growth with the same time constant of 3300 ± 300 fs (see Figure 3b). The similarity in the kinetics for several of the ionic species indicates that they are formed from common precursors.

In the previous study on femtosecond dynamics of transition metal hexacarbonyl photolysis, we observed pronounced coherent oscillations (period of 350 fs) in the long-lived transients.[8,9] Therefore, we carefully checked for similar behavior in the iron system. However, no oscillations were detected for $Fe(CO)_n^+$, $n = 2, 1, 0$ (Figure 3a). In an investigation of $Mn_2(CO)_{10}$ and $Re_2(CO)_{10}$, an anisotropy was found to decay due to electronic relaxation.[4,37] In $Fe(CO)_5$, the anisotropy was below 5% for all signals even at the earliest times and the time behavior of parallel and perpendicular signals did not differ.

A referee expressed his concern that the possibility to extract time constants from the pump−probe overlapping region may be controversial. The strong probe field could, in principle, modify the potential surfaces. The first two steps occurring during this time (section 4) could possibly be affected thereby. Therefore, we also checked for any dependence of the signal shapes on the probe-laser intensity, varying the latter by a factor

of 3. Attenuating the probe reduced the relative strength of the pedestal (late-time signal) of the light fragments. This observation is expected since ionization from the product ground state needs more probe photons, and hence depends on a higher power of the probe pulse energy, than ionization from an electronically excited state. However, the time constants had no detectable intensity dependence. Hence any influence of the strong field on the time constants seems to be negligible in this case. This conclusion is confirmed by the observation in $Mo(CO)_6$ and $W(CO)_6$ that identical lifetimes of the initially excited states of 30 and 46 fs, respectively, are evaluated from within and outside the pump−probe overlapping time, i.e., from the shift of the signal maximum and from the exponential tail, respectively.[8,9] We interpret the absence of any strong-field effect to the rates by the very large widths of the states or steep slopes of surfaces which are associated with the short lifetimes and which also express themselves in the broad absorption bands.

4. Simulation of the Kinetics

At early time (<300 fs) every fragment shows different temporal behavior. Hence there must be several different precursors before ionization. It seems appropriate to model the system by several consecutive precursors (levels, observation windows), each produced from the previous one by its own rate. In section 5, we discuss the nature of these levels; in particular, whether they are different species or only locations on the potential energy surface. We use kinetic equations with a minimum number of levels to simulate the signals. Parameters are the rate constants τ_{ij}^{-1} and the probabilities (cross sections) ${}^{M}\sigma_i$ for forming a specific ion M from level i. Note that more than one precursor level can contribute to a given fragment and each level can produce more than one ionic species.

Femtosecond transition-state spectroscopy with probing of a population during the different steps of the reaction was previously successfully described by kinetic equations.[38] Although a kinetic model ignores coherences, it is a powerful tool for providing insight into the population flow.

The simple preliminary analysis in the previous section already yields four time constants (21, 30, 47, and 3300 fs). The rate-equation simulation then provides an additional constant and, in particular, also the sequence of the processes. To simulate the ion signals, the solutions of the kinetic equations (i.e., the time-dependent populations of levels) are convoluted with the real pulse shape of the pump and probe pulses, as has been discussed elsewhere.[33−35,36] We found that the kinetics for all ions can be reproduced by six levels. This is depicted in Scheme 1, which also gives the number (m_i) of probe photons needed to produce the ions $Fe(CO)_k^+$ from each level i.

In Scheme 1, the first level (L_1) is the initially excited state of the parent molecule $Fe(CO)_5$ and the sixth level (L_6) is the final product of the UV photodecomposition. To cover the main features of the initial kinetics of all the fragments, we must introduce to Scheme 1 at least four intermediate levels L_2−L_5. In this scheme, the time constant τ_{ij} describes the lifetime of the ith level, which is determined by its decay to a consecutive level j. The parameter m_i shows the order of the ionization process from the ith level; it is used as the exponent of the probe intensity in the convolution integral. A larger m_i thus narrows down the instrumental function. But the effect is small for m_i in the range from 3 to 6. We use the values $m_i = 3, 3, 4, 5, 6, 6$ for $i = 1, ..., 6$, respectively. Three is the minimum number of probe quanta required to ionize the initially excited level L_1, and six the number to overcome the ionization potential

SCHEME 1: Rate-Equation Model for Simulation of Photochemical Decomposition of $Fe(CO)_5$

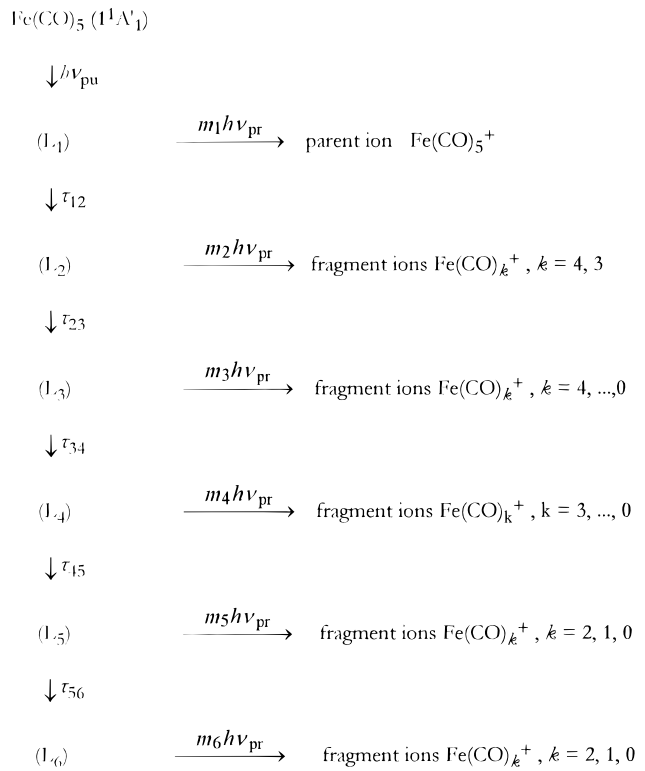

TABLE 1: Lifetimes τ_{ij} and Effective Ionization−Dissociation Cross Sections σ_{im} Used in the Six-Level Rate-Equation Model to Simulate the Dynamics[a]

level L_i	L_1	L_2	L_3	L_4	L_5	L_6
$\tau_{i,i+1}$/fs	21 ± 2 fs	15 ± 5	30 ± 3	47 ± 5	3300 ± 300	∞
$Fe(CO)_5^+$	1.000	0	0	0	0	0
$Fe(CO)_4^+$	0	0.924	0.076	0	0	0
$Fe(CO)_3^+$	0	0.517	0.452	0.032	0	0
$Fe(CO)_2^+$	0	0	0.677	0.252	0.038	0.032
$FeCO^+$	0	0	0.124	0.604	0.131	0.142
Fe^+	0	0	0.125	0.500	0.170	0.210

[a] σ_{im} (rows 3−9) represent effective cross sections to produce a specific ion m (first column) from a given level L_i (first row). $\Sigma_i \sigma_{im}$ is normalized to 1. The error limits given for the time constants $\tau_{i,i+1}$ correspond to the uncertainty of the time zero ($i = 1$), to the estimated range in which the simulation still fits reasonably well ($i = 2$), and the standard deviation of $\tau_{i,i+1}$ averaged over at least 10 runs ($i = 3$−5).

of any possible fragment. Table 1 gives the parameters with which the six-level rate-equation model well simulates the kinetics of all the ions. In Figures 2 and 3, the results of the simulation (solid lines) are compared with the experimental data.

In the simulation we tried to minimize the number of precursor levels for each signal and of the levels in total. Both the shape and position of the parent ion signal were found to be well simulated by the first level alone, with a lifetime $\tau_{12} = 21 \pm 2$ fs being used. (The error limit ±2 fs is determined not by the fitting procedure but by the uncertainty of the time zero.) The $Fe(CO)_4^+$ transient has a 30 fs decaying tail. But to reproduce this signal correctly, two levels with 21 and 30 fs lifetimes are not enough. One more short-lived (15 ± 5 fs) level L_2 has to be introduced to take into account both the 40 fs shift of the maximum and width of the signal. The kinetics of all other transient ion signals can be well described by introducing two more levels L_4 and L_5 with lifetimes of 47 and 3300 fs already derived in section 3 and the final product level L_6 with

infinite ($\geq$1 ns) lifetime, which takes into account the constant pedestal in the $Fe(CO)_n^+$, $n = 2, 1, 0$ signals.

It should be realized that the five time constants were *not* determined from a single time-resolved curve with multiexponential fitting; such a procedure would yield results which depend on each other. Instead, four of the constants (τ_{12}, τ_{34}, τ_{45}, τ_{56}) were derived from singly exponential fitting and one (τ_{23}) from triply exponential fitting with fixed τ_{12} and τ_{34} (in part with deconvolution) of independent signals. Furthermore, many of the constants were found in several signals; that is, they are based on redundant information. In contrast, the preexponential factors (ionization cross sections) are interdependent and furthermore depend on the probe intensity, as mentioned in the previous section. Therefore, their quantitative values are not used for conclusions.

5. Discussion

5.1. Probing Method. Probing was done by nonresonant (800 nm) photoionization. This has the advantage of giving rise to many different ionic fragments which, as the time dependence is different for every fragment, provides more information than, for instance, transient absorption in which typically only one electronic transition is probed. The different time behavior implies that the ionic fragments cannot have a common neutral precursor. Also, Bañares et al. observed (with two-photon pumping at 400 nm but other conditions comparable to ours) a multiple fragmentation pattern at early delay times;[6,7] they assumed that the fragmentation already occurred in the neutral molecule. However, the precursors are not necessarily different species but can also correspond to different states or locations on the potential energy surface. This was repeatedly demonstrated for molecules which exhibit no photochemical fragmentation at all, but nevertheless give rise to fragment ions (e.g., refs 33, 39, and 40). The cause of the ionic dissociation is excess energy, most of it originating from the vibrational energy of the neutral released on the way down the potential surface. This energy is conserved to a large part during the (vertical) photoionization.[33,35,36,41] The ions have much more time ($\leq$10 ns, given by the extraction process from the ion source and the associated peak width) than the neutrals (femtoseconds to picoseconds of observation time) to dissociate at a given excess energy.

In the simulation, the levels of the rate-equation model (see Scheme 1) correspond to observation windows on the potential surfaces of educt and products. The windows differ by their probabilities to produce a specific ion. The lifetimes correspond to an averaged time of travel through the window and departure from it. Whereas the kinetic analysis yields the time constants and the sequence of the consecutive processes, it does not automatically specify where exactly on the surface each window should be located. Assignment is facilitated, however, by the information on excess energy and thus on electronic energy (their sum is constant!) given by the fragmentation. If a neutral precursor $Fe(CO)_n$ has a vibrational energy exceeding the threshold for the ionic dissociation $Fe(CO)_n^+ \rightarrow Fe(CO)_{(n-k)}^+ + k$ CO, upon ionization it will yield no fragment heavier than $Fe(CO)_{(n-k)}^+$. (Whether it will also yield smaller fragments is commented below with reference to Fe^+.) The absence of $Fe(CO)_4^+$ and $Fe(CO)_3^+$ signals with delays longer than 300 fs can be explained by such post-ionization fragmentation. Typically, the parent ion is generated only by ionization from the Franck−Condon region and from locations where only little kinetic energy has been released, whereas the smallest fragment ions are observed after the neutral molecule has arrived at the ground state. Of course, ionization of the latter consumes more probe photons than that of the excited states (Scheme 1). This mechanism of fragmentation is only complicated by the fact that the ions can also absorb additional photons from the tail of the probe laser pulse and thus photodissociate. An obvious example of this kind is the formation of the atomic ion Fe^+, because the energy of a single pump photon is not sufficient to remove all the ligands either from the parent neutral or from the parent ion. Details of these processes have already been discussed.[8,33,35,36,42,43]

The large number of independent signals which are observed not only provides more information than typically in, e.g., transient absorption, but results in an effective time resolution which can be much below the pulse widths. If for instance two subsequent observation windows would give rise to one signal each, the temporal separation between the two signals and their delay versus the time zero could be measured with high accuracy (2 fs in our case), depending only on the signal-to-noise ratio. That is, these two consecutive processes are temporally resolved in this manner.

It is worth mentioning that the probe intensities used in this work are 10 times smaller than those previously used by us, e.g., with $Cr(CO)_6$,[8] although the ionization potentials are rather similar. The easy ionizability of $Fe(CO)_5$ with 800 nm light suggests the existence of a multiphoton resonance, probably at an energy around $2h\nu_{800\ nm} = 3.1$ eV. This would also be consistent with the observation in refs 6 and 7 of a long-lived parent-ion signal at negative delay times which is discussed in section 5.7.

5.2. Is There Any Synchronous CO Elimination? It seems reasonable to consider two eliminations to be synchronous (or "concerted"[44]) if they occur on a time scale much shorter than the period of an Fe−C stretch vibration (about 70 fs). The $Fe(CO)_5^+$ and $Fe(CO)_4^+$ signals disappear within 21 fs and 21 + 15 + 30 = 66 fs, respectively. If every ion signal corresponded to a neutral precursor of the same mass, this would imply a nearly synchronous process. However, a closer look at the data disproves this conclusion.

The parent $Fe(CO)_5^+$ and all heavy fragments $Fe(CO)_4^+$ and $Fe(CO)_3^+$ show clearly different time behavior. To reproduce these signals (see previous section), we had to postulate four different precursor levels (observation windows), L_1−L_4 (whose identity, species or location on the potential, is still to be assigned). For synchronous bond breaking, only two precursor levels would make sense, one before and one after the cleavage of the bonds. This simple consideration leaves no space for synchronous bond breaking.

Conclusive evidence comes from comparison with the photochemistry in solution, where only one CO is split off.[2,12] The cage effect, which is known to reduce the dissociation quantum yield to below 1 for metal carbonyls,[45,46] would never completely suppress any second dissociation, if it existed, and complexes such as $Fe(CO)_3S_2$ (S = solvent) should then be found in small yield. Since this has never been observed, a second CO seems not to be eliminated in solution. However, everything can be understood if the elimination of the first CO begins already in an electronically excited state, whereas the second step (and the following ones) begins only in the hot ground state. (It will turn out that it is actually the lowest singlet state. The real ground state is a triplet.) These later steps are prevented by cooling by the solvent. Vibrational cooling times are of the order of many picoseconds (section 5.5). So, *no reaction with a time constant well below 1 ps will be suppressed in solution,* and conversely, *"hot reactions", which are pre-*

vented in solution, must have time constants well above 1 ps in the gas phase. Hence, all the time constants below 50 fs in this work must be associated with the photochemical elimination of the first CO and the electronic relaxations connected with it. The same is probably true for the times ≤ 150 fs in the experiment of Bañares et al.[6,7] These authors used two-photon excitation at 400 nm.

Hence, we conclude that all our time constants but the last are connected with the photochemical reaction $Fe(CO)_5 \rightarrow Fe(CO)_4 + CO$. Only the last one (3.3 ps) can be due to elimination of a second CO. Let us discuss the steps one after the other.

5.3. The Processes Near the Franck−Condon Region. As discussed in section 5.1, the decay time τ_{12} of the parent ion signal represents the time of departure from the Franck−Condon region. Since there are quite a number of electronic states close by (see below), it seems plausible that the molecule changes over to one (or more) of them within this time. From the brevity (21 fs), we can immediately infer that intersystem crossing cannot be involved, just as not in the next three steps either. (In $HCo(CO)_4$, intersystem crossing has been calculated to take about 50 ps.[47]) Hence, we can exclude the pathway suggested on the basis of calculations that assumed initial intersystem crossing to the lowest excited triplet state before dissociation, which would then lead directly to the triplet ground state of $Fe(CO)_4$.[22] To understand more, let us consider the states which have been calculated quantum chemically.

Daniel and co-workers[22,29] report at least seven excited singlet states below 50 000 cm^{-1} not comprising Rydberg states (schematically indicated in the inset of Figure 4). Only three of them (species E′, E′, and A_2'') can be reached by symmetry-allowed transitions from the ground state. According to ref 29, the lowest excites state (1E′) is of d → d ("ligand field", LF) character and therefore carries little oscillator strength. The next two allowed transitions (to $1A_2''$ and 2E′) are of metal-to-ligand charge transfer (MLCT, $d \rightarrow \pi^*_{CO}$) type and are more intense. These two bands seem to overlap in the region of the pump wavelength (267 nm). If the MLCT character were pure, these states would not be repulsive along an Fe−CO coordinate due to Coulomb attraction. Interaction with repulsive LF states (note that the symmetry is reduced along the dissociation coordinate) lends them some repulsion too.[22] Recent calculations with the similar compound $H_2Fe(CO)_4$ show, however, that the slope is small and almost vanishes near the Franck−Condon region.[25] For the nondegenerate A_2'', the slope must even be zero along any Fe−CO coordinate due to symmetry equivalence of CO ligands. (The slope can also be not equal to 0 in the direction of a totally symmetric stretch. But such a coordinate can be ignored here since it would lead to simultaneous dissociation of several CO.)

Since the 2E′ MLCT state is degenerate, Jahn−Teller splitting should be taken into account. This effect predicts that the degeneracy will be lifted by distortion along a coordinate of e′ symmetry. One of the two resulting states will be stabilized, and the other destabilized. In $Fe(CO)_5$, there are four coordinates of e′ symmetry, two of them involving stretching of the equatorial Fe−C and C−O bonds, respectively, the other two involving C−Fe−C bending of the equatorial and axial ligands, respectively. Considering that an Fe−C bonding electron is excited, most likely the e′ stretch coordinate will be the largest component in the direction of steepest descent. This means that the molecule is initially accelerated in a direction which involves stretching of bonds to not only one but two to three of the equatorial ligands! In contrast to the slope in the direction of a Jahn-Teller active coordinate (which has unfortunately not yet been calculated), stretching of a single Fe−CO bond begins with a nearly (2E′) or exactly ($1A_2''$) horizontal slope on the potential energy surface, as mentioned. The ultrashort time (21 fs), which is only a fraction of a typical Fe−C stretching period (70 fs), is probably not compatible with an initial lack of acceleration (in a zero-slope direction). Hence, our results support the motion along the Jahn-Teller coordinate and that the pump laser predominantly populates the 2E′ state, much more than the $1A_2''$ state.

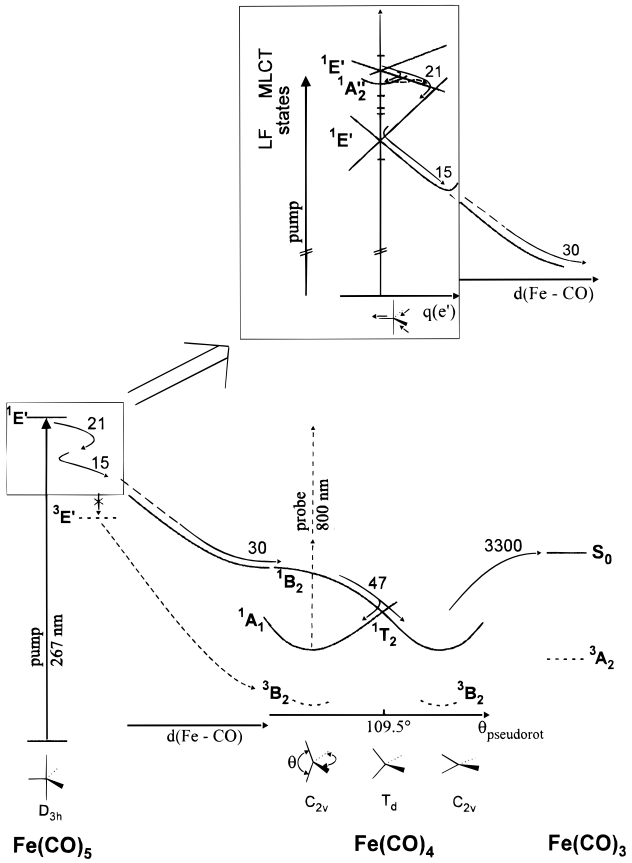

Figure 4. Scheme of the potential energy surfaces and pathways (times indicated near the arrows in femtoseconds) of the UV photodecomposition of $Fe(CO)_5$. Excited levels of the parent molecule[22,29] which are probably not involved in the process, are only indicated by short lines. The inset shows details of the processes in the parent molecule. The symmetry species ^{1}E′ in the inset designates the states before Jahn−Teller splitting, i.e., on the axis $q = 0$. The broken line in the inset indicates an $A_2'' \rightarrow E'$ pathway displaced along an e″ direction outside the drawing plane. The drawing is not to scale. The following energies (in electronvolts) of the product levels relative to the ground state of $Fe(CO)_5$ are derived from experimental dissociation energies[14] and, for the excited states, from calculations:[22,25,26] ($Fe(CO)_4$) $^3B_2$, 1.8; $^1A_1$, 2.56; $^1B_2$, 3.08; ($Fe(CO)_3$) $^3A_2$, 2.3; S_0, 3.5.

However, along the Jahn-Teller coordinate, we can expect an intersection between the two surfaces since the degenerate state is split, whereas the nondegenerate one will be bound along this coordinate (Figure 4, inset). The population can relax via this crossing to $1A_2''$ and can again leave from there by passing around this conical intersection (the path being displaced along an e″ direction) and then join again the direct relaxation path from 2E′, as indicated in the inset of Figure 4. All these processes can be extremely fast. Since the transition moment to the 2E′ state is in the equatorial plane, whereas that to $1A_2''$ is in the axial direction, such a sideway can explain why there was no anisotropy even at the earliest times.

It is worth noting that the Jahn-Teller splitting generates potential energy surfaces in the shape of a double cone with

the degenerate state at the apex. This is because the e′ coordinate is doubly degenerate so that the slopes are the same along every direction in this two-dimensional space.

Several of the Fe−CO antibonding ligand-field states were predicted to lie below the optically excited 2E′ level,[22,24,29] and the one with E′ symmetry was calculated to be even the lowest excited state.[24,29] It will again be subject to Jahn-Teller splitting along the same or a very similar e′ coordinate. The slopes will be steeper due to the stronger antibonding. This is schematically shown in Figure 4 (inset), which also indicates an intersection between the surface derived from this 1E′ level with that derived from the optically excited 2E′ level. This intersection will again be conical, with a branching space spanned by a pair of coordinates related to the e′ deformation. (The symmetry species results from the product of E′ with E′ and reduction to the lower symmetry group.[48])

The initial motion is now obvious (inset of Figure 4). The molecules in the optically populated state (2E′) are first distorted along an e′ coordinate involving stretching of more than one Fe−CO bond. Some of them will make an excursion to the $1A_2''$ state, but quickly return; then, they cross over to the ligand-field state 1E′ and temporarily return to the symmetric geometry. From there they go on along the same coordinate, but later on change direction to split off a single CO. The second time constant (15 fs) can naturally be attributed to the motion on the 1E′ surface. The third window (time constant 30 fs) probably begins long before dissociation is completed, most likely soon after the change of direction from the Jahn-Teller to a single-bond cleavage coordinate. This assignment is based on the following energy consideration.

In the third window, $Fe(CO)_4^+$ is still observed, although with small abundance (see the table). If this ion would be generated from neutral $Fe(CO)_4$ (i.e., if the window would begin only after dissociation), we must postulate that the unsaturated carbonyl is produced with a vibrational excess energy of less than 1.1 eV (equals dissociation energy of $Fe(CO)_4^+$ [32]). The available vibrational + kinetic energy after reaching the S_1 state of $Fe(CO)_4$ (see next section) is 1.6 eV, which is shared with the CO split off. If the latter carries 0.5 eV away, then ionization of $Fe(CO)_4$ could in fact yield its parent ion. Whereas this possibility cannot be excluded, consideration of finer details (such as a probable shift of the ionic versus the neutral potential surfaces) suggests that it is not very likely. The observation of $Fe(CO)_4^+$ can be more easily explained if the third window is opened in an energy range where dissociation is not yet complete.

Since the predicted sequence of states depends on the level of calculation (compare refs 22, 24, and 29), some details of this pathway may be subject to change. It may well be that other states and intersections will be involved in addition. For example, if it turned out that the degenerate ligand field state is above the optically populated one, the steep slope of the repulsive surface may result in intersection with the lower surface, just as in the case of the hexacarbonyls.[9] However, in any case, it is probably the Jahn−Teller effect and the interplay between the optically populated state with the repulsive ligand field state which drive the reaction, and the experiment tells that the molecule changes the electronic state and/or the direction of motion several times before it dissociates.

In the inset of Figure 4, we indicated another state below 1E′. It has not been predicted by the recent[29] and previous calculations. In our opinion, a long-lived state in this region must be postulated, however, to explain the long-lived (>10 ps) $Fe(CO)_5^+$ transient observed at negative delay times in ref 7 with pumping by two 800 nm photons. If this pump process populated the 1E′ level, the lifetime should be comparable with 15 fs (Figure 4); similarly, if the pump process involved three photons, it would populate the same state(s) as in our 267 nm excitation and would therefore again imply a very short decay, and with four photons, the same (short-lived) states would be populated as with the two 400 nm photons reported in ref 7 too. Hence, we claim that two-photon excitation at 800 nm populates an $Fe(CO)_5$ state which is long-lived and thus cannot involve ligand-field excitation. This resonance also explains why $Fe(CO)_5$ is (see end of section 5.1) much easier to ionize by 800 nm radiation than $Cr(CO)_6$, although the two molecules have very similar ionization energies.

5.4. The Steps After Photodissociation. $Fe(CO)_4$ has C_{2v} symmetry in its lowest singlet states S_0 ($1A_1$) and S_1 ($1B_2$)[26,27] as well as in its triplet ground state T_0 (1^3B_2).[49,50] Since S_0 of $Fe(CO)_4$ is nondegenerate, it can correlate only with the ground state of $Fe(CO)_5$. The lowest excited state of the latter must therefore correlate with the next higher singlet of $Fe(CO)_4$. This is in agreement with the quantum chemical calculations.[22] However, although $Fe(CO)_4$ is primarily generated in its S_1 state, luminescence has never been detected. For explanation, we suggest ultrafast internal conversion from S_1 to S_0 with a lifetime identical to our fourth time constant (47 fs). All this seems very similar to the case of $Cr(CO)_5$ (produced by dissociation of $Cr(CO)_6$), where we found an ultrafast internal conversion pathway from S_1 to S_0 via a Jahn-Teller-induced conical intersection.[8]

Hence, we should look for a degenerate state of $Fe(CO)_4$ in a symmetric geometry, where Jahn-Teller distortion will lead to correlation with both S_1 and S_0 in the C_{2v} geometry. $Fe(CO)_4$ in tetrahedral symmetry has a d electron configuration of e^4 t_2^4 giving rise to singlet states of species A_1, E, and T_2 and to a triplet $^3T_1$. The latter two are triply degenerate. Coordinates of species e and t_2 are Jahn−Teller active. Distortion along the e direction (angle deformation as indicated in the figure with opposite angles being equal) leads to the states A_1 and E in D_{2d}; further reduction of symmetry to C_{2v} results in the states A_1, B_2 (as needed), and B_1, the latter not being indicated in Figure 4. One-step deformation along a superposition of an e and a t_2 coordinate leads to the same result. This is how Ceulemans, Poliakoff, and co-workers described and analyzed in detail the Jahn−Teller effect in the triplet $^3T_1$ of tetrahedral $Fe(CO)_4$ leading to the ground state 1^3B_2 (and other states) in C_{2v}.[50,51] Hence, we suggest that the ultrafast internal conversion from the initially populated excited $1B_2$ to the lowest singlet state $1A_1$ of C_{2v} $Fe(CO)_4$ proceeds via a barrierless pathway through a Jahn−Teller-induced conical intersection at tetrahedral geometry (Figure 4). The motion of the ligand described by the abscissa (and by all combinations of the five Jahn−Teller active coordinates of the symmetries e and t_2) has been called non-Berry pseudorotation.[50] This internal ligand exchange is very much analogous to the case of $Cr(CO)_5$ (produced by photodissociation of the hexacarbonyl), where the pseudorotation is of the Berry type.[52] It is interesting that this type of vibration was manifested in $Cr(CO)_5$[8] and other group-6 pentacarbonyls[9] as a periodic oscillation of the probe signal. To explain the sensitivity of the probe to this vibration, we pointed to the fact that the S_0-S_1 resonance of $Cr(CO)_5$ is tuned along this coordinate from zero frequency (conical intersection) via the laser frequency (corresponding to 1.55 eV) to the final S_0-S_1 distance (about 2 eV). It is fully consistent with this interpretation that no oscillation was detected in $Fe(CO)_4$ since the (calculated) S_0-S_1 distance is only 0.52 eV[25] in this molecule.

5.5. The Slow Final Time Constant. The next time constant (3.3 ps) is nearly 2 orders of magnitude slower. Two processes can be considered for it: (1) slow electronic relaxation such as intersystem crossing and (2) a hot reaction such as dissociation of the next ligand, stimulated by the excess vibrational energy released on the way down to the product S_0.

Only the latter process can be suppressed in solution by collisional cooling, and only for this reaction will the rate depend on the excess energy and thus on the excitation wavelength. Weitz and co-workers found in an experiment with nanosecond time resolution with excitation at 351 nm in the gas-phase both singlet and triplet $Fe(CO)_4$.[18,19] Such a long lifetime rules out intersystem crossing taking place within picoseconds in this molecule. (See also the next section.) The 3.3 ps must hence be assigned to elimination of the second CO in the singlet manifold. The product singlet $Fe(CO)_3$ has also been identified by Weitz and co-workers in the gas phase.[18,19] It can, beyond the time range of 500 ps investigated by us, relax to its triplet ground state and subsequently, supported by the released energy, eventually lose another ligand.

The assignment as a dissociation driven by vibrational excess energy is in agreement with the observation that in solution elimination of a second CO is suppressed. This is expected if the time constant for collisional cooling is not much longer than that of the reaction. Deactivation times for low-frequency vibrations such as those of the Fe−C bonds are in the 10 ps range.[45,46] (Note that within one-tenth of the time constant, the temperature would decrease by 10%, a cooling which might already sufficiently slow the reaction.)

The time for elimination of the second CO in the chromium carbonyl system was found to be 0.93 ps.[8] In view of the small dissociation energy (0.43 eV[14]) of ground-state $Fe(CO)_4$, it seems surprising at first sight why the analogous reaction should take three times longer. However, it should be noted (1) that the dissociation energy of singlet $Fe(CO)_4$ is larger (about 0.94 eV, calculated from ground-state dissociation[14] and excitation[25,26] energies, according to ref 26 even >1.15 eV) than in the triplet, comparable to that of $Cr(CO)_5$, and (2) that the excess energy available in S_0 $Fe(CO)_4$ (about 2.0 eV minus the energy carried away by CO) is less than that in $Cr(CO)_5$ since S_0 is an excited state of $Fe(CO)_4$. RRKM calculations[14] at such excess energies give dissociation rates which are consistent with a time constant around 3 ps.

5.6. Intersystem Crossing. The early ab initio calculations[22−24] of Daniel and co-workers investigated the directly repulsive potential energy curve leading from the lowest triplet state ($1^3E'$) of $Fe(CO)_5$ to the triplet ground state of $Fe(CO)_4$, tacitly assuming that intersystem crossing (ISC) in $Fe(CO)_5$ is faster than dissociation. The latter is, however, very fast, so that ISC probably cannot compete (section 5.3). In the calculations, a singlet pathway was presented too, but with avoided crossings instead of conical intersections between the states. Such a path is necessary (at least in addition to a triplet path) to explain the formation of singlet $Fe(CO)_4$.[18,19] Weitz et al.[17] and Hepburn et al.[16] assumed that the singlet curves start from higher electronic states of $Fe(CO)_5$. In the calculations, the excited states are connected with the product states by simple repulsive curves.

Also, in the dissociation of $Cr(CO)_6$[8] and the other group 6 hexacarbonyls,[9] we found no indication of intersystem crossing even after elimination of the second CO. "No indication" means that all the steps can be assigned within the singlet pathway, including a coherent oscillation along a pseudorotation coordinate which would have no counterpart in the triplet manifold of the group 6 pentacarbonyls. On the other hand, there is no direct experimental evidence against the existence of an undetected parallel channel in the triplet manifold. In their careful work on time-resolved IR spectroscopy in gas-phase photolysis of $Fe(CO)_5$,[17−21] Weitz and co-workers observed both species, singlet and triplet $Fe(CO)_4$ (distinguished by their chemical reactions), at delays up to many tens of nanoseconds.[18,19] They presented evidence that both of them are primary products so that this photodissociation would proceed via at least two channels. The analysis was complicated by the fact that the spectra of the two species overlap to some extent and the spectral shapes are time-dependent due to cooling effects. We argue in favor of a pure singlet channel on the basis of time constants of competing processes.

Quantum chemically, it has been estimated that a triplet forms from the excited states of $H_2Fe(CO)_4$ with a rate of 0.35%/ps, corresponding to a time constant of 290 ps.[25] Similarly, for $HCo(CO)_4$, a time in the range of 50 ps was suggested.[47] In $Fe(CO)_4$, intersystem crossing (ISC) seems to take even nanoseconds, to judge by the delayed observation of singlet $Fe(CO)_4$ by Weitz and co-workers.[18,19] (This is beyond our observation time of 500 ps.) The collisional relaxation times presented by them suggest that ISC even needs more than 200 ns in $Fe(CO)_4$ and $Fe(CO)_3$. Excluding much heavier elements, the shortest time we know for ISC is 300 fs for excited $Ru(bipy)_3^{2+}$.[53] Even if the spin changed with such a fast rate also in the excited $Fe(CO)_5$, ISC would hardly be able to compete with the fast singlet-channel dissociation, which takes about 66 fs (= 21 + 15 + 30 fs) or even with the individual initial processes.

5.7. Further Comparison with Previous Work. The time for expulsion of a CO ligand from $H_2Fe(CO)_4$ after UV excitation has been calculated by quantum dynamics to take about 100 fs,[25] this being well consistent with our results on $Fe(CO)_5$. Upper bounds for the dissociation times have been deduced by Grant and co-workers from the yields of resonant two-photon ionization.[13] The resulting bounds (≤0.6 and 1 ps with excitation at 290 and 310 nm, respectively) are still too high. With our assignment, one must expect a *shorter* lifetime than measured at 267 nm, if the short-lived ligand-field state $1E'$ is directly excited at longer wavelength. On the other hand, if a level of even lower energy can be populated, the decay time can again be lengthened. This is apparently the case with two-photon excitation at 800 nm, to judge by the results of ref 7 at negative delay times.

Grant and co-workers also found an inverted vibrational population in the photochemically eliminated CO.[13] For explanation, they pointed to the decrease of the C−O distance on going from the complex to the free CO. However, the degree of vibrational excitation very much depends on how suddenly the distance will change; in other words, how abrupt is the turn of the valley in the surface in which the potential energy is plotted versus the C−O and Fe−C distances. While the required curvature is conceivable and one can also argue on a mechanical basis invoking the ultrafast acceleration along the Fe−C coordinate, which will transfer some momentum to the carbon atom, our mechanism offers a more attractive explanation: the pump laser excites a charge transfer state with a weakened CO bond; the system then suddenly jumps to the ligand field state with its restored CO distance which then further shortens during the rapid dissociation. Already in the first two transitions the CO vibration will be excited for Franck−Condon reasons.

Several statistical models have been suggested to describe the translational and rotational energy distributions over the fragments as measured in photofragment spectroscopy[16,14] and

SCHEME 2

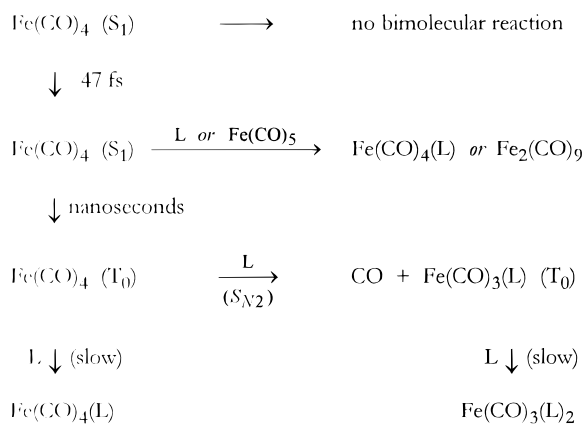

the abundance of the unsaturated metal carbonyl products.[15] For the expulsion of the second and following ligands, such models are justified. (However, they should take into account that the reactions take place in the hot S_0 state, not in the triplet ground states.) But the first CO is eliminated photochemically; that is, its kinetic energy is due to acceleration along the potential energy surfaces, and everything happens in a time much too short for attaining equipartition of energy. This step should be treated separately. Instead, the models comprised all the dissociation steps. The fact that they well reproduced the experiments means that in this system the product distribution and the rotational and translational energies are not sensitive to the mechanism. A clearly nonstatistical feature is the vibrational inversion in CO mentioned above. Nonstatistical product distributions were also found in experiments with nanosecond excitation, which probably involved several consecutive photochemical steps (see, for example, ref 11).

Nayak et al. found in $Fe(CO)_5$ photosubstitution of two CO's initiated by a single photon.[12] They proved that one of the new ligands L (such as a phosphine, pyridine, or (iso)nitriles) was introduced in a ground-state reaction in either of two ways: either in a substitution of $Fe_2(CO)_9$ formed at high $Fe(CO)_5$ concentrations by reaction with $Fe(CO)_4$ (S_0) or at high L concentrations in a substitution reaction in the triplet $Fe(CO)_4$. We can now substantiate this mechanism with the lifetimes for unimolecular decay (Scheme 2). Whereas the S_1 state of $Fe(CO)_4$ is much too short-lived (47 fs) to undergo any bimolecular reactions, the S_0 state has sufficient time (nanoseconds in solution) to insert into $Fe(CO)_5$ or to add an L. In the triplet ground state of $Fe(CO)_4$ (infinite lifetime) the reactant L can substitute one CO in a bimolecular reaction. (Instead of such an S_{N2} path, Nayak et al. suggested an addition−elimination mechanism.[12] However, the postulated triplet intermediate $^3Fe(CO)_4L$ would have too high an energy to be formed.) In a slower reaction, the triplet complexes with 4-fold coordination can also add an L with simultaneous intersystem crossing.

In light of the present results, it is also interesting to discuss a recent experiment[54] on "coherent control of chemical reactions" in which dissociative photoionization of $Fe(CO)_5$ and $CpFe(CO)_2Cl$ was used to maximize or minimize the ratio of two ion signals by tailoring the 800 nm femtosecond laser pulses; $Fe^+/Fe(CO)_5^+$ and $CpFeCOCl^+/FeCl^+$ varied by a factor of 70 and 4, respectively, depending on pulse shape and other details. In principle, pump−probe experiments could also be interpreted in terms of coherent control, in which the "product" (ion signal) depends on the delay time. (Alternatively, the leading front of the pulse in ref 54 varying in shape could be considered as a pump and the trailing edge as a probe.) In our experiment, the ratio $Fe^+/Fe(CO)_5^+$ varies by a factor of >200 (compare Figures 2a and 3a, restoring however a background of a few percent which was subtracted). We have shown that, except elimination of the first CO, fragmentation takes place only after ionization and is caused by excess vibrational energy or/and absorption of an additional photon. Any coherence within the ion can be expected neither for the thermal nor the secondary photochemical dissociation. The ion internal energy controlling the fragmentation can probably also be influenced by temperature or laser intensity. It is also known that in cyclopentadienyl (Cp) complexes the Cp ligand can be cleaved off only thermally.[2]

6. Concluding Remarks

Dissociation of the first CO of $Fe(CO)_5$ with its individual steps is remarkably fast. The sum of the first three time constants (21 + 15 + 30 fs) is below 100 fs. As argued in section 5.4, this implies that the acceleration already begins in the Franck−Condon region. This is not self-evident. If the excited state were nondegenerate, the potential energy curve along an Fe−CO dissociation coordinate would begin with zero slope since there are symmetry-equivalent ligands. Jahn-Teller splitting of a degenerate state, however, gives rise to a nonvanishing slope. It thus explains the initial fast acceleration and predicts that it involves more than one CO ligand. (Superposition with a totally symmetric stretch coordinate, which also involves several ligands, is not excluded.) Such a degenerate (2E′) state is available in the right wavelength region; due to its metal-to-ligand charge transfer character the corresponding absorption is intense and, due to its short lifetime (steep slope), also broad so that it can overlap with the pump wavelength. On the other hand, the nondegenerate $1A_2''$ MLCT state has also been predicted in this region.[29] To explain the lack of anisotropy, we also assume an intermediate population of the $1A_2''$ state (via the $2E'/1A_2''$ conical intersection) which then rapidly returns to the main relaxation path.

Jahn−Teller (JT) splitting also raises the probability of crossing with other potential energy surfaces. In particular, we suggested in section 5.4 an intersection with another JT-split surface with that of the lower-lying, strongly repulsive ligand field state 1E′. Without the splitting, there would be little chance of crossing with a lower-lying steeper surface; it would then be difficult to understand a time constant as short as 21 fs for conversion between two electronic states. Similar chains of JT-induced intersections have been found in the positive ions of benzene or of P_4 by Köppel.[55] In less symmetric molecules, the second-order Jahn-Teller effect of nearly degenerate states[56,57] can probably give rise to similar effects.

As already pointed out in section 5.2, it may turn out by computational progress that in the Franck−Condon region the strongly repulsive LF states lie higher than the initially excited one, in analogy to the situation in the group 6 hexacarbonyls.[58−61] Then an intersection or avoided crossing of the two surfaces can be expected due to the slope difference, as suggested for the case of $M(CO)_6$ dissociation.[8,9] The basic mechanism before dissociation would remain unchanged, however—initial acceleration along JT coordinates, repeated change of direction and electronic states via JT-induced conical intersections, and only thereafter transition to a steeply repulsive LF surface.

The change of electronic state and change of acceleration direction is in contrast to the textbook suggestion,[2] which assumed that the optical excitation directly populates the repulsive state.

In previous experiments with high-intensity nanosecond UV laser pulses, it has been suggested that resonant two-photon

excitation could populate states with energies above the ionization limit and that the neutral molecule subsequently loses all its ligands explosively.[62] However, the ultrafast dissociation found in this work hardly leaves time for absorption of a second photon with the pulses employed. Probably further excitation took place after dissociation.

The observed fast rates imply not only real crossings but also that they are accessible without barriers. In view of the closely spaced upper states, an absence of barriers is natural. In the dissociation product, we can conclude from the easy accessibility that the singlet T_2 state of tetrahedral $Fe(CO)_4$ lies energetically between the S_0 and S_1 states of the molecule in the equilibrium C_{2v} geometry. The fast rate through this conical intersection is also remarkable for another reason. As in all cases with a triply degenerate state, the intersection space is only $(f - 5)$-dimensional,[63] where $f = 23$ is the number of internal coordinates; the branching space is then 5-dimensional and is spanned by two e and three t_2 coordinates. The common case is 2-fold degeneracy with an $(f - 2)$-dimensional intersection space. Although it has been shown that a conical intersection presents no bottleneck for the molecular trajectories,[64] it is often asked whether the molecule can find such a small "point" ($(f - 2)$-dimensional space) as the tip of the cone. Our result shows that even an $(f - 5)$-dimensional space presents no problem. The reason is, of course, that the wave packet has a nonzero extension in f dimensions and can already cross over in the surrounding of the "point".

Acknowledgment. We are grateful to Robin N. Perutz for stimulating discussions.

References and Notes

(1) Wrighton, M. S. *Chem. Rev.* **1974**, *74*, 401.

(2) Geoffroy, G. L.; Wrighton, M. S. *Organometallic Photochemistry*; Academic Press: New York, 1979.

(3) Mcgregor, S. A.; Eisenstein, O.; Whittlesey, M. K.; Perutz, R. N. *J. Chem. Soc., Dalton Trans.* **1998**, 291.

(4) Kim, S. K.; Pedersen, S.; Zewail, A. H. *Chem. Phys. Lett.* **1995**, *233*, 500.

(5) Ihee, H.; Cao, J.; Zewail, A. H. *Chem. Phys. Lett.* **1997**, *281*, 10.

(6) Bañares, L.; Baumert, T.; Bergt, M.; Kiefer, B.; Gerber, G. *Chem. Phys. Lett.* **1997**, *267*, 141.

(7) Bañares, L.; Baumert, T.; Bergt, M.; Kiefer, B.; Gerber, G. *J. Chem. Phys.* **1998**, *108*, 5799.

(8) Trushin, S. A.; Fuss, W.; Schmid, W. E.; Kompa, K. L. *J. Phys. Chem. A* **1998**, *102*, 4129.

(9) Fuss, W.; Kompa, K. L.; Schmid, W. E.; Trushin, S. A. Femtosecond dynamics of photoinduced chemical reactions studied by intense-field dissociative ionization. In *AIP Conference Proceedings 454 (Proc. of the 9th Int. Symp. on Resonance Ionization Spectroscopy, Manchester, UK, June 1998)*; Vickerman, J. C., Lyon, I., Lockyer, N. P., Parks, J. E., Eds.; The American Institute of Physics: River Edge, NJ, 1998; p 163.

(10) Gutmann, M.; Janello, J. M.; Dickeboom, M. S.; Grossekathöfer, M.; Lindener-Roenneke, J. *J. Phys. Chem. A* **1998**, *102*, 4138.

(11) Yardley, J. T.; Gitlin, B.; Nathanson, G.; Rosan, A. M. *J. Chem. Phys.* **1981**, *74*, 370.

(12) Nayak, S. K.; Farrell, G. J.; Burkey, T. J. *Inorg. Chem.* **1994**, *33*, 2236.

(13) Whetten, R. L.; Fu, K.-J.; Grant, E. R. *J. Chem. Phys.* **1983**, *79*, 4899.

(14) Venkataraman, B. K.; Bandukwalla, G.; Zhang, Z.; Vernon, M. *J. Chem. Phys.* **1989**, *90*, 5510.

(15) Rubner, O.; Engel, V. *Chem. Phys. Lett.* **1998**, *293*, 485.

(16) Waller, I. M.; Hepburn, J. W. *J. Chem. Phys.* **1988**, *88*, 6658.

(17) Seder, T. A.; Ouderkirk, A. J.; Weitz, E. *J. Chem. Phys.* **1986**, *85*, 1977.

(18) Ryther, R. J.; Weitz, E. *J. Phys. Chem.* **1991**, *95*, 9841.

(19) Ryther, R. J.; Weitz, E. *J. Phys. Chem.* **1992**, *96*, 2561.

(20) Weitz, E. *J. Phys. Chem.* **1994**, *98*, 11256.

(21) Poliakoff, M.; Weitz, E. *Acc. Chem. Res.* **1987**, *20*, 408

(22) Daniel, C.; Benard, M.; Dedieu, A.; Wiest, R.; Veillard, A. *J. Phys. Chem.* **1984**, *88*, 4805.

(23) Veillard, A.; Strich, A.; Daniel, C. *Chem. Phys. Lett.* **1987**, *141*, 329.

(24) Marquez, A.; Daniel, C.; Sanz, J. F. *J. Phys. Chem.* **1992**, *96*, 121.

(25) Heitz, M.-C.; Daniel, C. *J. Am. Chem. Soc.* **1997**, *119*, 8269.

(26) Barnes, L. A.; Rosi, M.; Bauschlicher, C. W., Jr. *J. Chem. Phys.* **1991**, *94*, 2031.

(27) Li, Y.; Schreckenbach, G.; Ziegler, T. *J. Am. Chem. Soc.* **1995**, *117*, 486.

(28) Ehlers, A. W.; Frenking, G. *Organometallics* **1995**, *14*, 423.

(29) Rubner, O.; Engel, V.; Hachey, M. R.; Daniel, C. *Chem. Phys. Lett.* **1999**, *302*, 489.

(30) Kotzian, M.; Rösch, N.; Schröder, H.; Zerner, M. C. *J. Am. Chem. Soc.* **1989**, *111*, 7687.

(31) Norwood, K.; Ali, A.; Flesh, G. D.; Ng, C. Y. *J. Am. Chem. Soc.* **1990**, *112*, 7502.

(32) Ricca, A.; Bauschlicher, C. W., Jr. *J. Phys. Chem.* **1994**, *98*, 12899.

(33) Trushin, S. A.; Fuss, W.; Schikarski, T.; Schmid, W. E.; Kompa, K. L. *J. Chem. Phys.* **1997**, *106*, 9386.

(34) Trushin, S. A.; Fuss, W.; Schmid, W. E.; Kompa, K. L. *J. Phys. Chem. A* **1998**, *102*, 4129.

(35) Fuss, W.; Kompa, K. L.; Schikarski, T.; Schmid, W. E.; Trushin, S. A. *SPIE Proc.* **1998**, *3271*, 114.

(36) Fuss, W.; Schmid, W. E.; Trushin, S. A. *J. Chem. Phys.*, submitted.

(37) Trushin, S. A.; Fuss, W.; Schmid, W. E. In preparation.

(38) Pedersen, S.; Zewail, A. H. *Mol. Phys.* **1996**, *89*, 1455.

(39) Fuss, W.; Schikarski, T.; Schmid, W. E.; Trushin, S.; Kompa, K. L.; Hering, P. *J. Chem. Phys.* **1997**, *106*, 2205.

(40) Trushin, S. A.; Diemer, S.; Fuss, W.; Kompa, K. L.; Schmid, W. E. *Phys. Chem. Chem. Phys.* **1999**, *1*, 1431.

(41) Fuss, W.; Hering, P.; Kompa, K. L.; Lochbrunner, S.; Schikarski, T.; Schmid, W. E.; Trushin, S. A. *Ber. Bunsen-Ges. Phys. Chem.* **1997**, *101*, 500.

(42) Poth, L.; Zhong, Q.; Ford, J. V.; Castleman, A. W., Jr. *J. Chem. Phys.* **1998**, *109*, 4791.

(43) Zhong, Q.; Poth, L.; Castleman, A. W., Jr. *J. Chem. Phys.* **1999**, *110*, 192.

(44) Kim, S. K.; Pedersen, S.; Zewail, A. H. *J. Chem. Phys.* **1995**, *103*, 477.

(45) Dougherty, T. P.; Heilweil, E. J. *Chem. Phys. Lett.* **1994**, *227*, 19.

(46) Lian, T.; Bromberg, S. E.; Asplund, M. C.; Yang, H.; Harris, C. B. *J. Phys. Chem.* **1996**, *100*, 11994.

(47) Heitz, M.-C.; Ribbing, C.; Daniel, C. *J. Chem. Phys.* **1997**, 106, 1421.

(48) Herzberg, G. *Electronic Spectra and Electronic Structure of Polyatomic Molecules;* Molecular Spectra and Molecular Structure; Van Nostrand Reinhold: New York, 1966; Vol. 3.

(49) Poliakoff, M.; Turner, J. J. *J. Chem. Soc., Dalton Trans.* **1974**, 2276.

(50) Poliakoff, M.; Ceulemans, A. *J. Am. Chem. Soc.* **1984**, *106*, 50.

(51) Ceulemans, A.; Beyens, D.; Vanquickenborne, L. G. *J. Am. Chem. Soc.* **1984**, *106*, 5824.

(52) Burdett, J. K.; Grzybowski, J. M.; Perutz, R. N.; Poliakoff, M.; Turner, J. J.; Turner, R. F. *Inorg. Chem.* **1978**, *17*, 147.

(53) Damrauer, N. H.; Cerullo, G.; Yeh, A.; Boussie, T. R.; Shank, C. V.; McCusker, J. K. *Science* **1997**, *275*, 54.

(54) Assion, A.; Baumert, T.; Bergt, M.; Brixner, T.; Kiefer, B.; Seyfried, V.; Strehle, M.; Gerber, G. *Science* **1998**, *282*, 919.

(55) Köppel, H. *Z. Phys. Chem.* **1997**, *200*, 3.

(56) Englmann, R. *The Jahn−Teller effect in molecules and crystals*; Wiley: London, 1972.

(57) Bersuker, I. B. *The Jahn−Teller effect and vibronic interactions in modern chemistry*; Plenum: New York, 1984.

(58) Pierloot, K.; Tsokos, E.; Vanquickenborne, L. G. *J. Phys. Chem.* **1996**, *100*, 16545.

(59) Pollak, C.; Rosa, A.; Baerends, E. J. *J. Am. Chem. Soc.* **1997**, *119*, 7324.

(60) Baerends, E. J.; Rosa, A. *Coord. Chem. Rev.* **1998**, *177*, 97.

(61) Rosa, A.; Baerends, E. J.; van Gisbergen, S. J. A.; van Lenthe, E.; Groeneveld, J. A.; Snijders, J. G. *J. Am. Chem. Soc.* **1999**, *121*, 10356.

(62) Jackson, R. L. *Acc. Chem. Res.* **1992**, *25*, 581.

(63) Longguet-Higgins, H. C. *Proc. R. Soc. (London) A* **1975**, *344*, 147.

(64) Manthe, U.; Köppel, H. *J. Chem. Phys.* **1990**, *93*, 1658.